Environmental Research Letters

LETTER

Changes in climate extremes over West and Central Africa at 1.5 °C and 2 °C global warming

Arona Diedhiou[1,6,11], Adeline Bichet[1], Richard Wartenburger[2], Sonia I Seneviratne[2], David P Rowell[3], Mouhamadou B Sylla[4], Ismaila Diallo[5], Stella Todzo[6], N'datchoh E Touré[6], Moctar Camara[7], Benjamin Ngounou Ngatchah[8], Ndjido A Kane[9], Laure Tall[9] and François Affholder[10]

1 University of Grenoble Alpes, IRD, CNRS, Grenoble INP, IGE, F-38000 Grenoble, France
2 Institute for Atmospheric and Climate Science, ETH Zurich, Zurich, Switzerland
3 Met Office Hadley Centre, Fitzroy Road, EX1 3PB, Exeter, United Kingdom
4 WASCAL Centre of Competence, Ouagadougou, Burkina Faso
5 Department of Geography, University of California, Los Angeles (UCLA), CA 90095, United States of America
6 LAPAMF - African Centre of Excellence on Climate Change, Biodiversity and Sustainable Development / Université Félix Houphouët Boigny, Abidjan, Côte d'Ivoire
7 LOSEC, Université Assane Seck de Ziguinchor, Ziguinchor, Senegal
8 Université de Ngaoundere, Ngaoundere, Cameroon
9 Institut Sénégalais de Recherches Agricoles (ISRA), Dakar, Senegal
10 CIRAD, Montpellier, France
11 Author to whom any correspondence should be addressed.

E-mail: arona.diedhiou@ird.fr

Keywords: African climate, temperature extremes, precipitation extremes, climate change, global warming

OPEN ACCESS

RECEIVED
1 November 2017

REVISED
27 April 2018

ACCEPTED FOR PUBLICATION
11 May 2018

PUBLISHED
20 June 2018

Abstract

In this study, we investigate changes in temperature and precipitation extremes over West and Central Africa (hereafter, WAF domain) as a function of global mean temperature with a focus on the implications of global warming of 1.5 °C and 2 °C according the Paris Agreement. We applied a scaling approach to capture changes in climate extremes with increase in global mean temperature in several subregions within the WAF domain: Western Sahel, Central Sahel, Eastern Sahel, Guinea Coast and Central Africa including Congo Basin.

While there are several uncertainties and large ensemble spread in the projections of temperature and precipitation indices, most models show high-impact changes in climate extremes at subregional scale. At these smaller scales, temperature increases within the WAF domain are projected to be higher than the global mean temperature increase (at 1.5 °C and at 2 °C) and heat waves are expected to be more frequent and of longer duration. The most intense warming is observed over the drier regions of the Sahel, in the central Sahel and particularly in the eastern Sahel, where the precipitation and the soil moisture anomalies have the highest probability of projected increase at a global warming of 1.5 °C. Over the wetter regions of the Guinea Coast and Central Africa, models project a weak change in total precipitation and a decrease of the length of wet spells, while these two regions have the highest increase of heavy rainfall in the WAF domain at a global warming of 1.5 °C. Western Sahel is projected by 80% of the models to experience the strongest drying with a significant increase in the length of dry spells and a decrease in the standardized precipitation evapotranspiration index. This study suggests that the 'dry gets drier, wet gets wetter' paradigm is not valid within the WAF domain.

1. Introduction

After the 21st Conference of Parties in Paris (2015), the decision to hold global temperature increases to 'well below 2 degrees' and to pursue efforts to limit warming to 1.5 °C above pre-industrial levels focused the climate change debate on a temperature threshold rather than on carbon emissions or concentrations. Moreover, the agreement does not highlight the potential impact of these targets on local to regional scales and the implications of these global temperature thresholds have not been fully assessed at subregional

and country levels. Specifically, stakeholders and policy makers need robust information with respect to associated changes on a regional scale, in particular for extreme events and the impact on humans and ecosystems (Oettli *et al* 2011, Seneviratne *et al* 2016, Schleussner *et al* 2016, Guiot and Cramer 2016, James *et al* 2017).

Here, we investigate changes in temperature and precipitation extremes over the West and Central Africa subregions for an increase of global mean temperature of 1.5 °C and 2 °C above the pre-industrial period, based on Seneviratne *et al* (2016) and as a follow-up to Wartenburger *et al* (2017). West and Central Africa are particularly threatened by climate change due to high climate variability, high reliance on rain-fed agriculture and limited economic and institutional capacity to respond to climate variability and change (Sultan and Gaetani 2016). It is thus particularly crucial to know if changes in the dominating climatological parameters in these subregions will be amplified with increasing global mean temperature. Furthermore, it is important to know whether the rate of these regional changes will allow for incremental adaptation, or whether it involves non-linear transformations, which require early mitigation to avoid unmanageable changes (James and Washington 2013).

James *et al* (2014) provided information for mitigation debates in analyzing temperature and precipitation changes in Africa associated with 1 °C, 2 °C, 3 °C and 4 °C of global warming. They showed that there is only little significant precipitation change at 1 °C, which becomes more pronounced the higher the global mean temperature. Chadwick *et al* (2016) show that the models provide confidence that many tropical regions will experience large changes in rainfall, but often disagree on the pattern of change. Nevertheless, the mean signal for Africa can be further decomposed into projections that a majority of the models suggest a wet signal in East Africa, and a drying signal in southern Africa, Guinea Coast and the West of the Sahel. Despite the uncertainties associated with these projections, an increase in risks associated with a 2 °C or higher degree of global warming clearly stands out.

Seneviratne *et al* (2016) focused on temperature and precipitation extremes in emissions scenarios and identified that changes in precipitation intensity are linearly linked to the changes in global mean temperature for almost all the different emissions scenarios. Vogel *et al* (2017) showed that projected changes at regional level will be amplified over most land areas due to strong control by soil moisture-temperature feedbacks.

In this study, we apply a scaling approach to capture the implications of variations of global mean temperature of 1.5 °C and 2 °C in changes of temperature and precipitation extremes in several subregions over West and Central Africa: western Sahel, central Sahel, eastern Sahel, Guinea Coast and Central Africa including Congo Basin. Data and methods are presented in section 2. The results of changes in climate extremes are presented in section 3 and the discussion and conclusion are presented in section 4.

2. Data and methods

2.1. Empirical sampling approach

Numerous approaches have recently been developed for identifying regional climate signals associated with specific global warming targets (James *et al* 2017). We here apply a hybrid approach that cannot be categorized into the four main techniques described in James *et al* 2017. We refer to it as the empirical sampling approach, which has been applied in Seneviratne *et al* 2016 and described in more detail in Wartenburger *et al* 2017. In contrast to pattern scaling (e.g. Tebaldi and Arblaster 2014, Lopez *et al* 2014), this approach does not need *a priori* assumptions about the nature of the dependency on global temperature (or other climate variables; e.g. Frieler *et al* 2012, Lynch *et al* 2016, Kravitz *et al* 2017) such as the linearity of the response (e.g. Fischer *et al* 2014). For predefined regions, this method derives the empirical dependency of changes in regional quantities as a function of global mean temperature changes based on a range of climate model projections (Herger *et al* 2015, Seneviratne *et al* 2016). The scatter plots of the scaling relationship between changes in global mean temperature (ΔTg) and in regional climate indices are computed as follows (see further detail below, in the description of the plots). Annual global mean temperatures are derived from each ensemble member and individual years before performing the 20 year moving average that we assign to the median year and then we compute the anomalies relative to the pre-industrial reference period 1861–1880. Over the land points, we do the same computation for the temperature and precipitation extreme indices averaged regionally. We will also assess the significance of this dependency relationship, against a null hypothesis of no relationship. To test this, we fit an ordinary least squares between changes in global temperature and in climate indices averaged regionally over land points, applied for each individual model realization for $\Delta Tg >= 1$ °C. The number of models for which the dependency relationship approximated by a linear regression is significantly different from zero ($p = 0.01$) will be shown in the discussion section to give an idea of robustness (Benjamini and Hochberg 1995).

The advantage of this approach is to provide in a single figure information on the response of a given regional quantity for different global mean temperature, on empirical assessment of this relationship (allowing e.g. to identify possible non-linearities), and on the range of inter-model and inter-scenario uncertainties. Box plots have been computed to capture the uncertainties between the models.

Table 1. List of climate indices (in alphabetical order). Star (*) denotes indices discussed but not shown in this paper.

Index	Description	Definition	Unit
CDD	Consecutive dry days	Maximum number of consecutive days with RR<1 mm	days
CSDI*	Cold spell duration indicator	Annual count of days with at least six consecutive days when TN<10th percentile	days
CWD	Consecutive wet days	Maximum number of consecutive days with RR>=1 mm	days
DTR	Diurnal temperature range	Annual mean difference between TX and TN	°C
P-E*	Precipitation—evaporation	Precipitation—evapotranspiration (Greve and Seneviratne 2015)	mm day^{-1}
PRCPTOT	Annual total wet-day precipitation	Annual total PRCP in wet days (RR>=1 mm). PRCPTOT is expressed in percent changes relative to the pre-industrial reference period 1861–1880.	mm
R1 mm*	Number of wet days	Annual count of days when RR >=1 mm	days
R99ptot	Contribution from very wet days	Annual total PRCPTOT when RR >99th percentile	mm
SMA*	Soil moisture anomalies	Soil moisture anomalies (Orlowsky and Seneviratne, 2013) no unit	1
SPEI12	Standardized precipitation evapotranspiration index	Standardized precipitation index based on 12 month accumulation period (Vicente-Serrano *et al* 2010); no unit	1
T	Mean temperature	Temperature at 2 m	°C
TNN*	Minimum of daily minimum temperature	Annual minimum value of daily minimum temperature	°C
TXX*	Maximum of daily maximum temperature	Annual maximum value of daily maximum temperature	°C
TX90p	Warm days	Percentage of days when TX>90th percentile	% days
WSDI	Warm spell duration indicator	Annual count of days with at least six consecutive days when TX>90th percentile	days

2.2. Data

The regional-scale dependencies between global mean temperature and a range of climate change indices (consisting of 11 indices from the joint CCl/CLIVAR/JCOMM Expert Team on Climate Change Detection and Indices (ETCCDI; Sillmann *et al* 2013a, 2013b), plus three additional water cycle indices computed by Wartenburger *et al* 2017, see table 1) are derived from global climate model (GCM) simulations performed within the frame of the Coupled Model Intercomparison Project Phase 5 (CMIP5, Taylor *et al* 2012). The subset of the CMIP5 models used in this study is identical to the model subset used in Wartenburger *et al* 2017 (table 1 therein). The regional changes are analyzed at the spatial scale typical of the models. To assess the impact of intra-model spread, we use only one ensemble member per model (r1i1p1). To assign the same weight to all simulations, all GCM output has been bi-linearly interpolated to a horizontal resolution of 2.5° × 2.5° prior to performing the empirical sampling analysis. Wartenburger *et al* (2017) have studied the natural variability in investigating the spread among all ensemble members of a particular model. They found that the model spread has essentially no impact on the ensemble mean or median, and even the spread is almost similar. Rowell (2012) showed that the role of natural variability is small in this region.

We consider for this study the yearly anomalies (relative to the pre-industrial reference period 1861–1880) of global mean temperatures ΔTg and the respective anomalies of the aforementioned indices computed for all emission scenario from each ensemble member and for all models. This reference period has also been used in previous publications that apply the scaling approach (Wartenburger *et al* 2017 and Seneviratne *et al* 2016). To be compatible with those studies (and to enhance comparability), it has been decided to stick to the same reference period here.

All indices and the global mean temperatures are smoothed by applying a 20 year moving average over land points of the West Africa region (WAF; Giorgi and Francisco 2000, hereafter referred to as the WAF domain) and over land points of smaller-scale regions located within the WAF domain (figure 1): western Sahel (WSA): 10°N–20°N/−18°W–10°W; central Sahel (CSA): 10°N–20°N/10°W–10°E; eastern Sahel (ESA): 10°N–20°N/10°E–30°E; Guinea Coast (GC): 5°N–10°N/10°W–10°E; Central Africa (including Congo Basin; CAF): 7.5°S–10°N/10°E–30°E.

The limitation with the WAF domain is that it mixes several climatic and ecological zones. Also, this region is facing a multitude of issues in terms of adaptation and mitigation (Redelsperger *et al* 2006). These regions have different landscapes and surface conditions (arid and semi-arid areas with savanna and trees over Sahel (WSA, CSA and ESA), forest over GC and equatorial forest in CAF with complex interactions with the West African monsoon. Due to substantial differences in their location relative to the tropical Atlantic and to the Hadley cell, those regions are characterized by very diverse hydrometeorological regimes. The mean annual precipitation in these regions is 575 mm in WSA, 450 mm in CSA, 347 mm in ESA, 1250 mm in GC and 2000 mm in CAF. Besides, the seasonality of precipitation in these regions is different with two

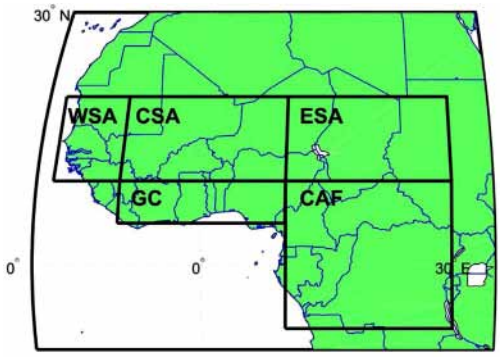

Figure 1. Map with borders of the WAF subregions: CAF, including Congo Basin;: −7.5°S to 10°N/10°E–30°E; WSA: 10°N–20°N/−18°W to −10°W; CSA: 10°N–20°N/−10°W–10°E; ESA: 10°N–20°N/10°E–30°E; GC: 5°N–10°N/−10°W to 10°E.

rainy seasons over GC, while the Sahel (WSA, CSA and ESA) is characterized by only one wet season (Sultan *et al* 2013).

2.3. Description of the plots

The plots below are computed from the CMIP5 simulations of one ensemble member r1i1p1 of all models available for 1961–2099 for each scenario (26 models for the scenarios 'Historical' and 'RCP8.5', 16 for RCP6.0, 23 for RCP4.5 and 19 for RCP2.6).

The scaling plots show the changes in climate indices in the WAF domain and WAF subregions with global mean temperature. Each color represents the multimodel mean of the corresponding scenario. The gray shading represents the minimum and maximum values simulated by the 110 (26+26+16+23+19) projections.

The boxplots represent the distribution of the 84 individual ensemble members for RCP8.5 (26 models), RCP6.0 (16 models), RCP4.5 (23 models) and RCP2.6 (19 models). For these plots, the scaling plots are the 20 year averages of the indices for which the respective 20 year average global mean temperature exceeds (or reaches) 1.5 °C (2 °C) for the first time.

In each boxplot, the central mark indicates the median value. The bottom and top edges of the box indicate the first and third quartile, respectively. The whiskers extend to the most extreme data points not considered outliers (that is any value comprised between the first (third) quartiles and 1.5* the interquartile range). The outliers (that is any value lower (higher) than 1.5* the interquartile range) are plotted individually using the |'+'| symbol.

3 Results

3.1. Changes in temperature extremes

The verification of the scaling of the temperature values is done in comparing the modeled (26 CMIP5 historical simulations, one member per model) scaling with observation-based (GSWP3) scaling for the period 1920–2010 (using a reference period of 1961–1990). To test our results against independent data, we have applied the same methodology to compute ETCCDI indices derived from the 3rd phase of the Global Soil Wetness Project (GSWP3, http://hydro.iis.u-tokyo.ac.jp/GSWP3/) forcing data set, which is the successor to GSWP2 (Dirmeyer *et al* 2006). We have opted for this recently developed data set, as it has gained high popularity in the modeling community and provides high-resolution (daily) estimates of climate variables back to 1900. Due to its limited temporal coverage, we use the period 1961–1990 as a reference for this comparison.

Figure 2 shows the verification of the scaling of temperature values from the CMIP5 models (HIST, in black) and observations (GSWP3, in red) for the ETCCDI indices (top to bottom, respectively) ΔTAS (hereafter ΔT as mean air temperature at 2 m), ΔDTR, ΔTX90p, ΔWSDI against global temperature ΔT_g averaged across the subregions: WSA, CSA, ESA, GC and CAF. Both models and observations show an increase in temperature, but the warming is around 1 °C in HIST and 2 °C in GSWP3 confirming that the models likely underestimate the temperature rise (Sherwood *et al* 2014). Except over CAF, ΔDTR decreases with temperature rising both in the models and in the observations. In all the subregions, ΔTX90P increases with temperature both in the models and in the observations. ΔWSDI increases with temperature rising mainly over the Sahel band (WSA, CSA and ESA) both in the models and observations, but over GC and CAF the models underestimate the magnitude and rate of change with temperature.

Figure 3 shows the scaling plot of ΔTg and changes in temperature (ΔT) for the WAF domain and the five subregions. The box plots show the responses at a global warming of 1.5 °C (hereafter ΔTg1.5C) and of 2 °C (hereafter ΔTg2C). The linear increase of regional temperatures with global mean temperature is confirmed whatever the size of the domain, with the regional projections for a specific global temperature increase marked by a relatively narrow ensemble spread (Engelbrecht *et al* 2015). Note, however, that if one takes the perspective of limiting carbon emissions, rather than specifying a temperature target, then modeling uncertainty is substantially enhanced (see the analysis of Rowell *et al* 2016 for Africa). Nevertheless, from either perspective, larger regional warming than global warming is highly likely. For the WAF region, a global warming of 1.5 °C (2 °C) induces a multi-model mean increase of 1.7 °C (2.3 °C). This warming is more intense in the driest regions of Sahel (CSA and ESA) where a ΔTg1.5C (ΔTg2C) is associated with a warming of 2 °C (2.7 °C) over CSA and of 1.9 °C (2.6 °C) over ESA. Over WSA, GC and CAF, the rates are weaker. We also note that the annual maximum of daily maximum temperature (ΔTXX, not shown) is projected to increase more rapidly than

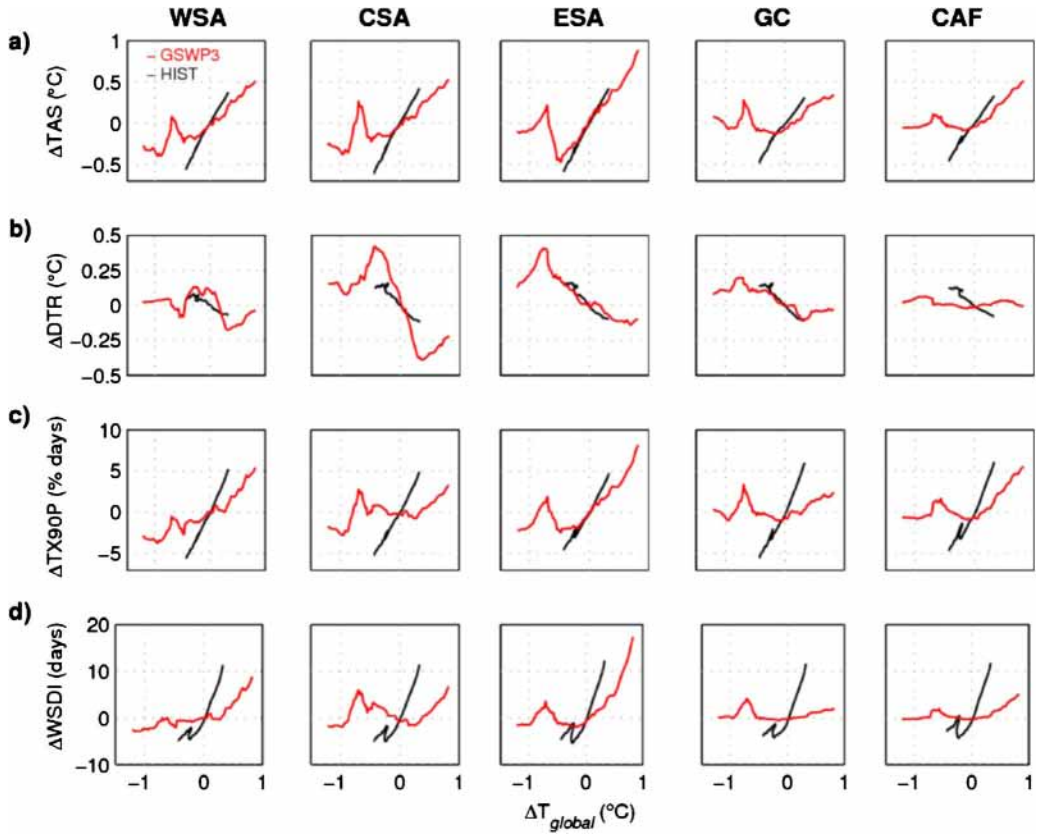

Figure 2. Scaling plots of ETCCDI temperature indices and global temperature values for the period 1920–2010 (compared to the reference period 1961–1990) from CMIP5 models (HIST, in black) and observations (GSWP3, in red). Top to bottom, respectively, for indices ΔTAS, ΔDTR, ΔTX90p, ΔWSDI (in *y* axis labels) against global temperature ΔT_g (in *x* axis labels) averaged across the subregions: WSA, CSA, ESA, GC and CAF.

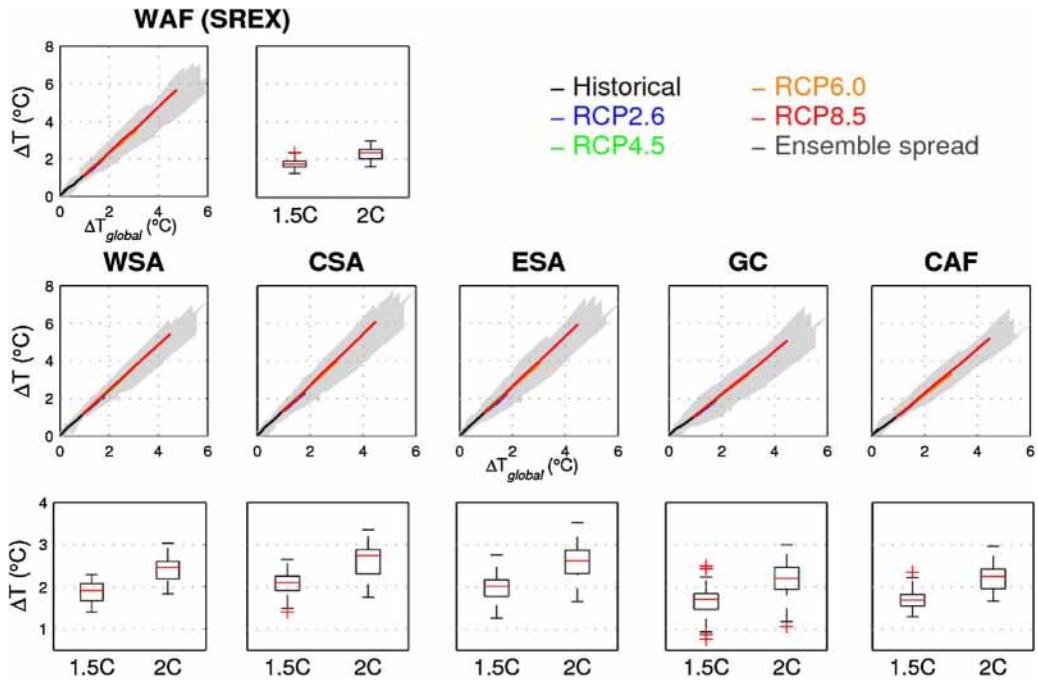

Figure 3. Scaling plots and box plots for 1.5 °C and 2 °C global mean temperature warming. Top and middle row: scaling plots of Δ*Tg* against regional temperature Δ*T* (in y axis labels) averaged across the WAF domain (top) and all of its subregions: WSA, CSA, ESA, GC and CAF. Bottom row: regional responses of Δ*T* to a global temperature increase of 1.5 °C and 2 °C. Upper and lower hinges of the box plots represent the first and third quartile. Whiskers extend to the highest (lowest) value that is within 1.5 times the interquartile range of the upper (lower) hinge. Central line of each box plot indicates the median value. Values outside this range are displayed as crosses (+).

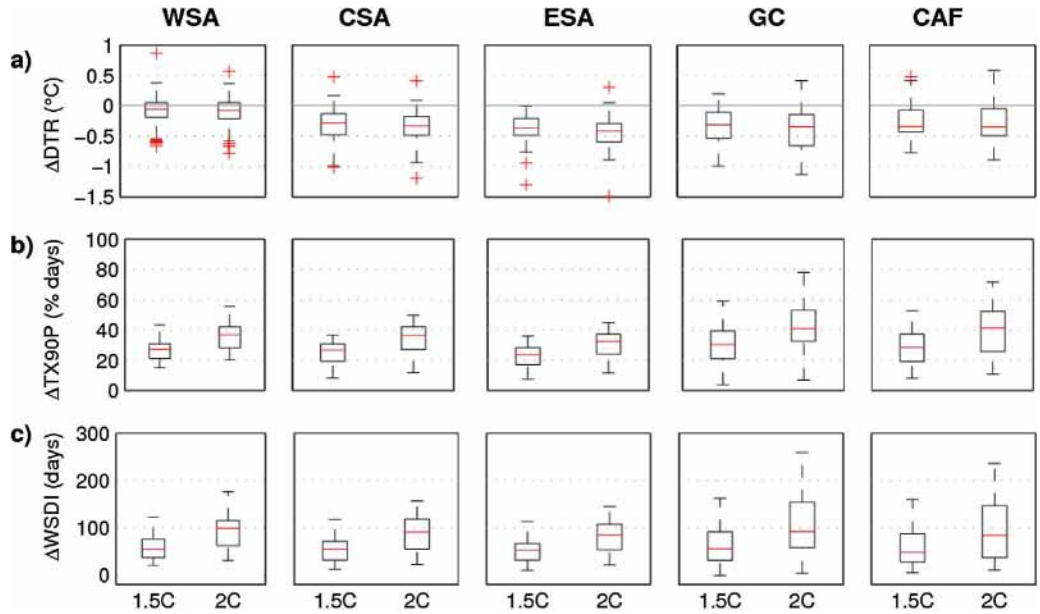

Figure 4. Regional responses of ΔDTR (top), ΔTX90p (middle) and ΔWSDI (bottom) for all WAF subdomains (columns) to a global temperature increase of 1.5 °C and 2 °C. Upper and lower hinges of the box plots represent the first and third quartile. Whiskers extend to the highest (lowest) value that is within 1.5 times the interquartile range of the upper (lower) hinge. Central line of each box plot indicates the median value. Values outside this range are displayed as crosses.

the global mean temperature with a particularly large magnitude over the Sahel. The annual minimum of daily minimum temperature (ΔTNN, not shown) in all subregions is projected to increase with ΔTg at even higher magnitudes than ΔTXX.

Figure 4 shows the box plots of the responses of the diurnal temperature range (ΔDTR, top), percentage of very hot days (ΔTX90P, middle), and of the warm spell duration index (ΔWSDI, bottom) to a $\Delta Tg1.5C$ and $\Delta Tg2C$ in the WAF subregions. The changes of the diurnal temperature range in all the WAF subregions present a disparity in the sign with a large spread either side of zero. However, at $\Delta Tg1.5C$, most models (62.5% of models in WSA, 95% in CSA, 100% in ESA, 93.8 in GC and 82.3% in CAF) projected a decrease ΔDTR with increase of ΔTg. We verified that this trend is mainly associated with the projected increase of the daily minimum temperature in most models (ΔTNN, not shown). The least pronounced changes are found over WSA, while the magnitudes in the other regions are similarly moderate.

There is a large spread across models for changes in above-average days, but in general the warmest areas of Sahel are projected to have the weakest increase of very hot days, while the wetter regions of GC and CAF are projected to experience the largest changes in ΔTX90p. The trend of the warm spell duration index (ΔWSDI) is similar to the trend of ΔTX90p with a large spread across the ensemble models. GC and CAF are projected in most of the models to have the longest warm spells. We note also that the cold spell duration index (ΔCSDI, not shown) is projected to decrease with increase of global temperature until a threshold of around $\Delta Tg = 2$ °C and remains constant thereafter. However, there is a large ensemble spread that is weaker in the drier subregions of Sahel and very large in the wetter areas of the domain.

As illustrated in figures 3 and 4, a 2 °C target for ΔTg implies increases in warm temperature extremes exceeding 2 °C in the WAF subregions. This may be due to the changes in the West African monsoon dynamic associated with land–sea contrast (Sutton *et al* 2007) in response to radiative forcing, or to feedbacks from decreases in soil moisture (Serreze and Barry 2011, Seneviratne *et al* 2013), which may further amplify changes in extreme temperatures in some of the regions (Seneviratne *et al* 2014). Higher temperatures expected in $\Delta Tg1.5C$ and $\Delta Tg2C$ will cause crops to grow faster, with thus less time for photosynthesis and then less biomass built per year. When occurring at specific development stages of most grain crops, very high temperature may severely reduce or even completely destroy the harvest of grain crops (Rosenzweig *et al* 2014, Varhammar *et al* 2015, Ahmed *et al* 2015). The increase of the frequency and intensity of warm spells will have serious implications for agriculture and human health (Weiss *et al* 2014, D'amato *et al* 2015, Partanen *et al* 2018).

3.2. Changes in precipitation extremes

Figure 5 shows the scaling plot of ΔTg and changes in total precipitation accumulated during wet days (ΔPRCPTOT) for the WAF domain and the five subregions. The box plots show the responses at $\Delta Tg1.5C$ and $\Delta Tg2C$. Although anomalies, and hence inter-model spread, tend to be slightly larger at the larger

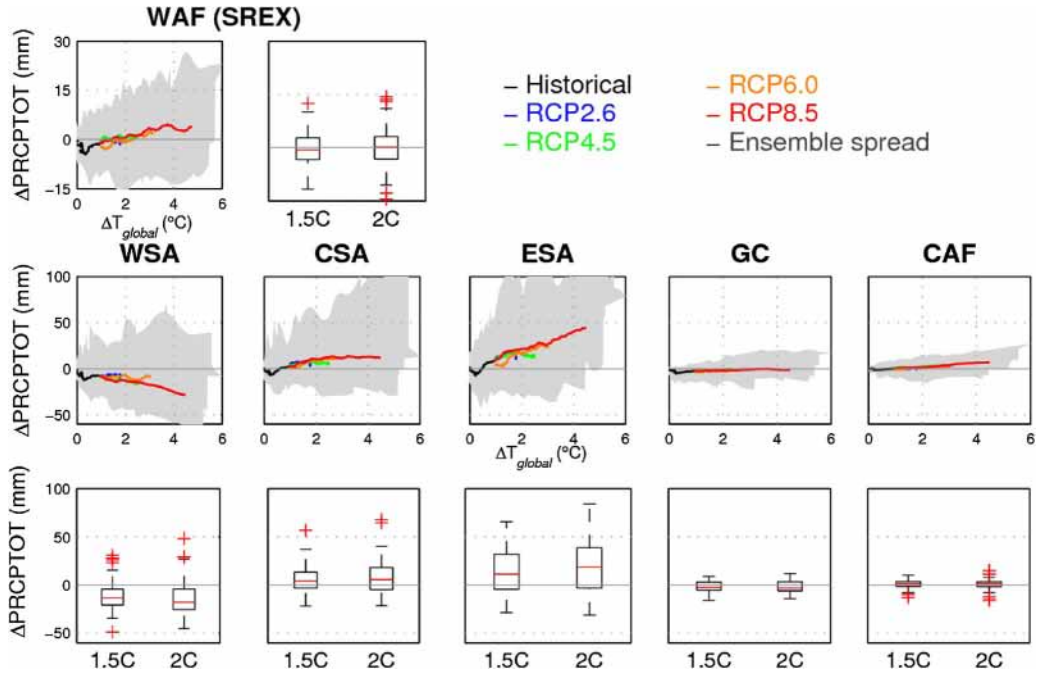

Figure 5. As for figure 2, but for changes in regional total precipitation (ΔPRCPTOT).

Table 2. Percentage of models showing an increase (above 0), respectively, at 1 °C and 2 °C global warming for all the subregions.

	ΔPRCPOT		ΔSPI12		ΔR99ptot		ΔCWD		ΔCDD	
	Δ*T*g1.5 °C	Δ*T*g2 °C	Δ*T*g1.5 °C	Δ*T*g2 °C	Δ*T*g1.5 °C	Δ*T*g2 °C	Δ*T*g1.5 °C	Δ*T*g2 °C	Δ*T*g1.5 °C	Δ*T*g2 °C
WSA	18.7	20.2	13.4	18.5	58.7	56.5	11.2	18.8	80	81.1
CSA	63.7	63.7	50	54.2	71.2	63.7	17.5	18.8	47.5	53.6
ESA	66.2	71	62.1	68.5	73.7	79.7	36.2	28.9	32.5	39.1
GC	36.2	31.8	37.8	31.4	77.5	72.4	15	17.3	53.7	62.3
CAF	63.7	66.6	58.5	62.8	87.5	85.5	25.9	24.2	41.2	44.9

warming target, it has previously been shown that at a specific time point each model's global warming has little impact on its regional precipitation change (Rowell 2012) in contrast to the strong impact seen above on regional temperature change. Hence, the model spread amongst wet day projections is large. Furthermore, more heterogeneous trends emerge when investigating changes over smaller scales, and so the spread is larger over these regions than for the WAF domain. Projections in the Sahel have a large spread. However, as shown in table 2, in most of the models, precipitation is projected to increase in the CSA and ESA (respectively for 63.75% of the models and for 66.25% at Δ*T*g1.5C), while a tendency of decrease of rainfall is noted over WSA (81.25% at Δ*T*g1.5C). This is in agreement with Diallo *et al* (2012), who suggested that drought conditions over WSA could likely be related to a delay in the onset of the wet season accompanied by an overall shortening of this period. Small changes are noted over the humid tropical and subtropical regions of GC and over CAF which have the weakest ensemble spread.

Figure 6 shows the box plots of the responses of the Standard Precipitation Evapotranspiration Index (ΔSPEI12) of annual total precipitation explained by very heavy precipitation greater that the 99 percentile (ΔR99PTOT), of maximum length of consecutive wet days (ΔCWD), and of maximum length of consecutive dry days (ΔCDD) at Δ*T*g1.5C and Δ*T*g2C. Mean changes in ΔSPEI12 at Δ*T*g1.5C and Δ*T*g2C are small and projections have a large spread in all the subregions. However, table 2 shows that in most of the models ΔSPEI12 is projected to increase with global temperature over ESA and CAF, while over WSA it is projected to decrease (respectively, at Δ*T*g1.5C for 62.19% of the models in ESA, for 58.5% in CAF and for 86.6% in WSA). This is in line with precipitation changes. Changes in ΔR99PTOT at Δ*T*g1.5C and Δ*T*g2C over Sahel (WSA, CSA and ESA) have a large spread among the models. However, it is computed in table 2 that most of the models projected an increase of the contribution of heavy rainfall in CSA and ESA (respectively, 71.2% and 73.7% of the models at Δ*T*g1.5C). The highest positive changes tend to be projected to be in GC and CAF (respectively, for 77.5% of the models and 87.5% at Δ*T*g1.5C), but these subregions are where the ensemble spread is the largest. Mean changes in ΔCWD at Δ*T*g1.5C and Δ*T*g2C are not pronounced over Sahel (WSA, CSA and ESA), but as shown in table 2, in most of the models ΔCWD is projected to decrease (88.8% of the models over WSA, 82.5% over CSA and 63.8% over ESA). The highest ensemble spread

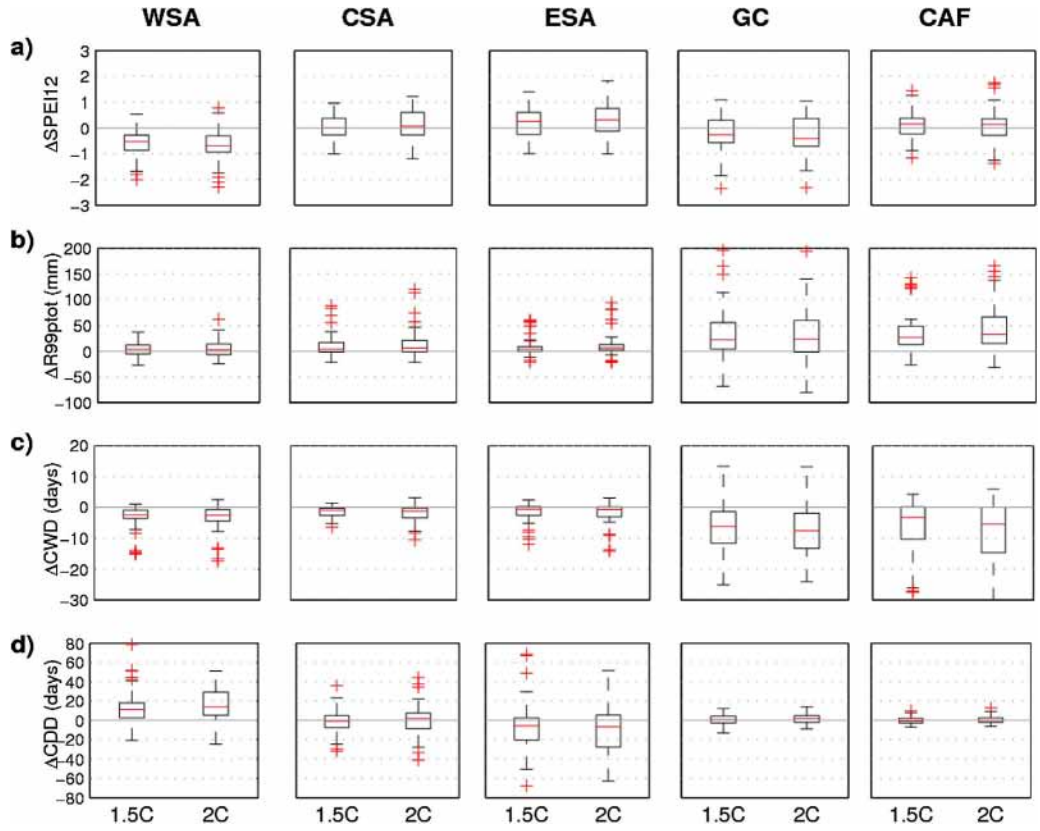

Figure 6. As for figure 3, but for regional responses of water cycle related indices (rows from top to bottom: SPEI12, R99ptot, CWD and CDD).

is found over GC and CAF where most of the models (85% in GC and 74.1% in CAF) projected a decrease of ΔCWD. There are uncertainties in the projections of the ΔCDD. However, ΔCDD is often projected to have the highest changes in the WSA with most of the models (80% of the models at Δ*T*g1.5C) projecting an increase of the maximum length of dry spells with Δ*T*g. Projections of ΔCDD in the CSA and ESA are not pronounced and there is a large ensemble spread, in contrast to projections in GC and CAF where the responses are not pronounced, but where the ensemble spread is the weakest.

In summary, while there are several uncertainties represented by the large ensemble spread of the models, most of models projected a decrease of total precipitation (81.25% of the models) over WSA, an increase of the length of dry spells (80% of the models) and a decrease of SPEI12 (86.6% of the models). Over central Sahel, eastern Sahel and CAF, most of the models (between 70% and 85% of the models) projected a regime of more heavy rainfall and less frequent rainy days for both temperature targets, in agreement with Sylla *et al* (2015) and Diallo *et al* (2016). The wetter subregions of GC and CAF are the areas where the ensemble spreads of projected precipitation related indices are the highest. However, most of the models projected a small change in precipitation (PRCPTOT) with a decrease of the maximum length of consecutive wet days (CWDs, between 75% and 85% of the models), of SPEI12 (60% in GC and 40% in CAF) and an increase in the contribution of heavy rainfall (between 77% and 87% of the models).

4. Discussion and conclusion

Table 3 displays the significant linear trends of the indices in the RCP8.5 scenario for Δ*T*g >=1 °C. The models generally agree that changes in global mean temperatures will enhance changes of regional-scale temperature extremes and that the length of warm spells will increase rapidly. The changes in the diurnal temperature range are more negative over the driest and warmest areas of the Sahel (CSA and ESA). A likely decrease of rainfall (PRCPTOT) is noted in the WSA with a decrease of the length of CWDs, an increase of the length of the consecutive dry days (CDDs) and an increase of the dryness; precipitation–evaporation (P–E). Likely increase of rainfall is noted in ESA with an increase of R1 mm, of SPEI12, of the contribution of very wet days (R99PTOT) and of the soil moisture (SMA). In agreement with Greve *et al* (2014) and Greve and Seneviratne (2015), the increase of rainfall and soil moisture over ESA found in this study does not confirm the 'dry gets drier, wet gets wetter' paradigm within our subregions (Held and Soden 2006, Chou *et al* 2009,

Table 3. Scaling slopes of the RCP8.5 scenario for $\Delta T >= 1$ °C and percentage of models with a statistically significant linear scaling (in brackets, $p = 0.01$) for the five subregions of the WAF domain. Unit of index is [X/°C], with X = unit of the index, which is provided in table 1.

Index [X/°C]	WSA	CSA	ESA	GC	CAF
ΔT/Δ*Tg*	1.21 (100)	1.37 (100)	1.33 (100)	1.15 (100)	1.18 (100)
ΔDTR/Δ*Tg*	−0.06 (38)	−0.13 (69)	−0.18 (92)	−0.10 (50)	−0.07 (54)
ΔWSDI/Δ*Tg*	68.47 (100)	65.92 (100)	57.81 (100)	69.36 (100)	68.56 (100)
ΔPRCPTOT/Δ*Tg*	−4.71 (50)	1.94 (19)	7.91 (38)	0.49 (19)	1.96 (62)
ΔR1 mm/Δ*Tg*	−2.21 (69)	−0.90 (42)	0.48 (27)	−2.08 (50)	−1.83 (54)
ΔSPEI12/Δ*Tg*	−0.25 (58)	0.01 (19)	0.19 (58)	0.04 (31)	0.22 (62)
ΔR99ptot/ Δ*Tg*	4.40 (19)	7.26 (31)	8.20 (50)	19.52 (58)	28.82 (85)
ΔCWD/Δ*Tg*	−0.80 (69)	−0.67 (54)	−0.28 (35)	−2.51 (54)	−2.90 (77)
ΔCDD/Δ*Tg*	13.40 (38)	1.46 (15)	1.24 (0)	−0.52 (19)	0.09 (15)
ΔP-E/Δ*Tg*	−0.01 (44)	−0.00 (4)	0.01 (8)	0.02 (32)	0.06 (48)
ΔSMA/Δ*Tg*	0.17 (19)	0.40 (31)	0.53 (50)	0.01 (42)	0.08 (50)

Seneviratne *et al* 2010). The wet regions of GC and CAF are projected to experience small changes in SMA and precipitation, while the contribution of very wet days is larger than in the drier areas of the Sahel.

Over CSA and ESA the model tendency to a projected increase of precipitation is associated with an increase in the trend of wet extremes. An increase of the contribution of heavy rainfall and of water availability may likely lead to an increase of flood cases and associated damage and costs in the subregion (Le Cozannet *et al* 2015, Avila *et al* 2016, Taylor *et al* 2017). Over GC and CAF the models tend to project a small increase of precipitation with an increase of the contribution of heavy rainfall and a decrease in the duration of wet spells. This suggests that more floods and landslide cases are likely to be expected above 1.5 °C (Gariano and Guzzetti 2016, Jacobs *et al* 2017). Moreover, increased rainfall intensity is likely to increase runoff and soil erosion, with a long-term negative impact on yields through nutrient losses (Sultan 2012, Sultan *et al* 2013). Western Sahel is projected to more likely experience the strongest drying at $\Delta Tg1.5C$, with a significant increase in the length of dry spells and a decrease in SPEI12. Above 2 °C, this region could become more vulnerable to drought as well as to heat waves and could encounter serious food security issues, since increased water stress will translate into decreased crop yields and production in a region where crops are predominantly rainfed and no land is available for increasing the cropping area (Rosenzweig *et al* 2014, Connolly-Boutin and Smit 2016, Ahmed *et al* 2015). This may be a potential hotspot for future drought-related changes (Sultan 2012, Orlowsky and Seneviratne 2013, Sultan *et al* 2014, Guiot and Cramer 2016, Schleussner *et al* 2016, Diallo *et al* 2016). The wide-ranging changes of climate extremes at 1.5 °C global warming could have an impact on water resources (availability, accessibility and demand) that may lead to problems with agriculture and food security. However, there is a need for further investigation to confirm the potential impact on key sectors of the sustainable development of the West and Central countries.

In conclusion, in this study we have applied an empirical sampling approach to capture changes in climate extremes with a global increase of temperature of 1.5 °C and 2 °C in smaller-scale regions within the West African SREX domain (WAF, SREX 2012). The temperature extremes within this region are projected to be higher than the global mean temperature increase, with the most intense warming observed over the Sahel. Heat waves are expected to be more frequent and of longer duration, with serious implications for human health and agriculture (Russo *et al* 2016). While there are several uncertainties and large ensemble spread in the projections of precipitation related indices, most of the models highlight large trends at sub-regional scale. In the majority of models, precipitation is projected to increase with increasing global mean temperature over CSA and ESA, and at a slower rate over GC and CAF. The trend in precipitation over CSA and ESA is associated with an increase in the trend in wet extremes. Over GC and CAF, a slight change of precipitation is projected with a significant increase of the contribution of heavy rainfall and a decrease in the duration of wet spells. WSA is generally projected to experience the strongest drying, as indicated by the significant increase in ΔCDD and the decrease in SPEI12. Nevertheless, significant uncertainties remain, including the possibility of shared biases amongst the models, future emissions policies, and limitations in the scaling due to internal variability and larger contribution of local processes such as aerosols, land-use and land-cover change (Lenton *et al* 2008, Flato *et al* 2013, Sutton *et al* 2015). Communication to policy makers therefore remains a critical challenge that the scientific community must continue to urgently address.

Acknowledgments

The research leading to this publication was co-funded by the NERC/DFID 'Future Climate for Africa' programme under the AMMA-2050 project, grant No. NE/M019969/1 and by the ANR project ACASIS (2014–17; Grant ANR-13-SENV-0007) on heat waves warning over Sahel. The authors acknowledge S I Seneviratne and R Wartenburger (funded by ERC DROUGHT-HEAT, grant agreement No. 617518) for providing the data for this analysis. Finally, we acknowledge the CCI/CLIVAR/JCOMM Expert Team

on Climate Change Detection and Indices (ETCCDI) and the World Climate Research Programme's Working Group on Coupled Modelling, which is responsible for CMIP, and we thank the climate modeling groups involved in this international program for producing and making available their model output. CMIP, the US Department of Energy's Program for Climate Model Diagnosis and Intercomparison provided coordinating support and led the development of the software infrastructure in partnership with the Global Organization for Earth System Science Portals.

ORCID iDs

Arona Diedhiou https://orcid.org/0000-0003-3841-1027
Richard Wartenburger https://orcid.org/0000-0003-4470-5080

References

Ahmed K F, Wang G, Yu M, Koo J and You L 2015 Potential impact of climate change on cereal crop yield in West Africa *Clim. Change* **133** 321–34
Ávila A, Justino F, Wilson A, Bromwich D and Amorim M 2016 Recent precipitation trends, flash floods and landslides in southern Brazil *Environ. Res. Lett.* **11** 114029
Benjamini Y and Hochberg Y 1995 Controlling the false discovery rate: a practical and powerful approach to multiple testing *J. R. Stat. Soc.* **57** 289–300
Chadwick R, Good P, Martin G and Rowell D P 2016 Large rainfall changes consistently projected over substantial areas of tropical land *Nat. Clim. Change* **6** 177–82
Chou C, Neelin J D, Chen C-A and Tu J-Y 2009 Evaluating the Rich-Get-Richer mechanism in tropical precipitation change under global warming *J. Clim.* **22** 1982–2005
Connolly-Boutin L and Smit B 2016 Climate change, food security, and livelihoods in sub-Saharan Africa *Reg. Environ. Change* **16** 385–99
D'amato G, Vitale C, De Martino A, Viegi G, Lanza M, Molino A and D'amato M 2015 Effects on asthma and respiratory allergy of climate change and air pollution *Multi. Respir. Med.* **10** 39
Diallo I, Giorgi F, Deme A, Tall M, Mariotti L and Gaye A T 2016 Projected changes of summer monsoon extremes and hydroclimatic regimes over West Africa for the twenty-first century *Clim. Dyn.* **47** 3931–54
Diallo I, Sylla M B, Giorgi F, Gaye A T and Camara M 2012 Multi-model GCM-RCM ensemble-based projections of temperature and precipitation over West Africa for the early 21st century *Int. J. Geophys.* **2012** 1–19
Dirmeyer P A, Gao X, Zhao M, Guo Z, Oki T and Hanasaki N 2006 GSWP-2: multimodel analysis and implications for our perception of the land surface *Bull. Am. Meteorol. Soc.* **87** 1381–98
Engelbrecht F, Adegoke J, Bopape M J, Naidoo M, Garland R, Thatcher M and Gatebe C 2015 Projections of rapidly rising surface temperatures over Africa under low mitigation *Environ. Res. Lett.* **10** 085004
Fischer E M, Sedlacek J, Hawkins E and Knutti R 2014 Models agree on forced response pattern of precipitation and temperature extremes *Geophys. Res. Lett.* **41** 2014GL062018
Flato G *et al* 2013 Climate change 2013: the physical science basis *Contribution of Working Group I to the Fifth Assessment Report of the Intergovernmental Panel on Climate Change* ed T F Stocker *et al* (Cambridge: Cambridge University Press) pp 741–866
Frieler K, Meinshausen M, Mengel M, Braun N and Hare W 2012 A scaling approach to probabilistic assessment of regional climate change *J. Clim.* **25** 3117–44
Gariano S L and Guzzetti F 2016 Landslides in a changing climate *Earth Sci. Rev.* **162** 227–52
Giorgi F and Francisco R and 2000 Uncertainties in regional climate change prediction: a regional analysis of ensemble simulations with the HADCM2 coupled AOGCM *Clim. Dyn.* **16** 169–82
Greve P, Orlowsky B, Mueller B, Sheffield J, Reichstein M and Seneviratne S I 2014 Global assessment of trends in wetting and drying over land *Nat. Geosci.* **7** 716–21
Greve P and Seneviratne S I 2015 Assessment of future changes in water availability and aridity *Geophys. Res. Lett.* **42** 5493–9
Guiot J and Cramer W 2016 Climate change: the 2015 Paris Agreement thresholds and Mediterranean basin ecosystems *Science* **354** 465–68
Held I M and Soden B J 2006 Robust responses of the hydrological cycle to global warming *J. Clim.* **19** 5686–99
Herger N, Sanderson B M and Knutti R 2015 Improved pattern scaling approaches for the use in climate impact studies *Geophys. Res. Lett.* **42** 3486–94
Jacobs L, Dewitte O, Poesen J, Maes J, Mertens K, Sekajugo J and Kervyn M 2017 Landslide characteristics and spatial distribution in the Rwenzori Mountains, Uganda *J. Afr. Earth Sci.* **134** 917–30
James R and Washington R 2013 Changes in African temperature and precipitation associated with degrees of global warming *Clim. Change* **117** 859–72
James R, Washington R and Rowell D P 2014 African climate change uncertainty in perturbed physics ensembles: implications of global warming to 4 °C and beyond *J. Clim.* **27** 4677–92
James R, Washington R, Schleussner C-F, Rogelj J and Conway D 2017 Characterizing half-a-degree difference: a review of methods for identifying regional climate responses to global warming targets *Wiley Interdiscipl. Rev. Clim. Change* **8** e457
Kravitz B, Lynch C, Hartin C and Bond-Lamberty B 2017 Exploring precipitation pattern scaling methodologies and robustness among CMIP5 models *Geosci. Model Dev. Discuss.* **10** 1889–902
Le Cozannet G, Raucoules D, Wöppelmann G, Garcin M, Da Sylva S, Meyssignac B and Lavigne F 2015 Vertical ground motion and historical sea-level records in Dakar (Senegal) *Environ. Res. Lett.* **10** 084016
Lenton T M *et al* 2008 Tipping elements in the Earth's climate system *Proc. Natl Acad. Sci. USA* **105** 1786–93
Lopez A, Suckling E B and Smith L A 2014 Robustness of pattern scaled climate change scenarios for adaptation decision support *Clim. Change* **122** 555–66
Lynch C, Hartin C, Bond-Lamberty B and Kravitz B 2016 Exploring global surface temperature pattern scaling methodologies and assumptions from a CMIP5 model ensemble *Geosci. Model Dev. Discuss.* (https://doi.org/10.5194/gmd-2016-170)
Oettli P, Sultan B, Baron C and Vrac M 2011 Are regional climate models relevant for crop yield prediction in West Africa? *Environ. Res. Lett.* **6** 014008
Orlowsky B and Seneviratne S I 2013 Elusive drought: uncertainty in observed trends and short- and long-term CMIP5 projections *Hydrol. Earth Syst. Sci.* **17** 1765–81
Partanen A I, Landry J S and Matthews H D 2018 Climate and health implications of future aerosol emission scenarios *Environ. Res. Lett.* **13** 024028
Redelsperger J L, Thorncroft C, Diedhiou A, Lebel T, Parker D J and Polcher J 2006 African monsoon multidisciplinary analysis (AMMA): an international research project and field campaign *Bull. Am. Meteorol. Soc.* **87** 1739–46
Rosenzweig C, Elliott J, Deryng D, Ruane A C, Müller C, Arneth A and Neumann K 2014 Assessing agricultural risks of climate change in the 21st century in a global gridded crop model intercomparison *Proc. Natl Acad. Sci.* **111** 3268–73

Rowell D P 2012 Sources of uncertainty in future changes in local precipitation *Clim. Dyn.* **39** 1929–50
Rowell D P, Senior C A, Vellinga M and Graham R J 2016 Can climate projection uncertainty be constrained over Africa using metrics of contemporary performance? *Clim. Change* **134** 621–33
Russo S, Marchese A F, Sillmann J and Immé G 2016 When will unusual heat waves become normal in a warming Africa? *Environ. Res. Lett.* **11** 054016
Schleussner C F, Lissner T K, Fischer E M, Wohland J, Perrette M, Golly A and Mengel M 2016 Differential climate impacts for policy-relevant limits to global warming: the case of 1.5 °C and 2 °C *Earth Syst. Dyn.* **7** 327–51
Seneviratne S I, Corti T, Davin E L, Hirschi M, Jaeger E B, Lehner I and Teuling A J 2010 Investigating soil moisture–climate interactions in a changing climate: a review *Earth Sci. Rev.* **99** 125–61
Seneviratne S I, Donat M, Mueller B and Alexander L V 2014 No pause in the increase of hot temperature extremes *Nat. Clim. Change* **4** 161–3
Seneviratne S I, Donat M G, Pitman A J, Knutti R and Wilby R L 2016 Allowable CO_2 emissions based on regional and impact-related climate targets *Nature* **529** 477–83
Seneviratne S I *et al* 2013 Impact of soil moisture-climate feedbacks on CMIP5 projections: first results from the GLACE-CMIP5 experiment *Geophys. Res. Lett.* **40** 5212–7
Serreze M C and Barry R G 2011 Processes and impacts of Arctic amplification. A research synthesis *Glob. Planet. Change* **77** 85–96
Sherwood S C, Bony S and Dufresne J L 2014 Spread in model climate sensitivity traced to atmospheric convective mixing *Nature* **505** 37
Sillmann J, Kharin V V, Zhang X, Zwiers F W and Bronaugh D 2013a Climate extremes indices in the CMIP5 multimodel ensemble: Part 25 1. Model evaluation in the present climate *J. Geophys. Res.* **118** 1716–33
Sillmann J, Kharin V V, Zwiers F W, Zhang X and Bronaugh D 2013b Climate extremes indices in the CMIP5 multimodel ensemble: Part 2. Future climate projections *J. Geophys. Res.* **118** 2473–93
SREX 2012 Managing the risks of extreme events and disasters to advance climate change adaptation *A Special Report of Working Groups I and II of the IPCC* ed C B Field *et al* (Cambridge: Cambridge University Press) p 582
Sultan B, Janicot S and Diedhiou A 2003 The West African monsoon dynamics, Part I: intraseasonal variability *J. Clim.* **16** 3389–406
Sultan B 2012 Global warming threatens agricultural productivity in Africa and South Asia *Environ. Res. Lett.* **7** 041001
Sultan B and Gaetani M 2016 Agriculture in West Africa in the twenty-first century: climate change and impacts scenarios, and potential for adaptation *Front. Plant Sci.* **7** 1262
Sultan B, Guan K, Kouressy M, Biasutti M, Piani C, Hammer G L and Lobell D B 2014 Robust features of future climate change impacts on sorghum yields in West Africa *Environ. Res. Lett.* **9** 104006
Sultan B, Roudier P, Quirion P, Alhassane A, Muller B, Dingkuhn M and Baron C 2013 Assessing climate change impacts on sorghum and millet yields in the Sudanian and Sahelian savannas of West Africa *Environ. Res. Lett.* **8** 014040
Sutton R, Suckling E and Hawkins E 2015 What does global mean temperature tell us about local climate? *Phil. Trans. R. Soc. A* **373** 20140426
Sutton R T, Dong B and Gregory J M 2007 Land/sea warming ratio in response climate change: IPCC AR4 model results and comparison with observations *Geophys. Res. Lett.* **34** L02701
Sylla M B, Giorgi F, Pal J S, Gibba P, Kebe I and Nikiema M 2015 Projected changes in the annual cycle of high-intensity precipitation events over West Africa for the late twenty-first century *J. Clim.* **28** 6475–88
Taylor C M, Belušić D, Guichard F, Parker D J, Vischel T, Bock O and Panthou G 2017 Frequency of extreme Sahelian storms tripled since 1982 in satellite observations *Nature* **544** 475
Taylor K E, Stouffer R J and Meehl G A 2012 An overview of CMIP5 and the experiment design *Bull. Am. Meteorol. Soc.* **93** 485–98
Tebaldi C and Arblaster J M 2014 Pattern scaling: Its strengths and limitations, and an update on the latest model simulations *Clim. Change* **122** 459–71
Varhammar A, Wallin G, McLean C M, Dusenge M E, Medlyn B E, Hasper T B and Uddling J 2015 Photosynthetic temperature responses of tree species in Rwanda: evidence of pronounced negative effects of high temperature in montane rainforest climax species *New Phytol.* **206** 1000–12
Vicente-Serrano S M, Beguería S and López-Moreno J I 2010 A multiscalar drought index sensitive to global warming: the standardized precipitation evapotranspiration index *J. Clim.* **23** 1696–718
Vogel M M, Orth R, Cheruy F, Hagemann S, Lorenz R, Hurk B J J M and Seneviratne S I 2017 Regional amplification of projected changes in extreme temperatures strongly controlled by soil moisture-temperature feedbacks *Geophys. Res. Lett.* **44** 1511–9
Wartenburger R, Hirschi M, Donat M G, Greve P, Pitman A J and Seneviratne S I 2017 Changes in regional climate extremes as a function of global mean temperature: an interactive plotting framework *Geosci. Model Dev.* **10** 3609
Weiss D J, Bhatt S, Mappin B, van Boeckel T P, Smith D L, Hay S I and Gething P W 2014 Air temperature suitability for plasmodium falciparum malaria transmission in Africa 2000–2012: a high-resolution spatiotemporal prediction *Malar. J.* **13** 171